Differentiating Different Subsidence Mechanisms in the Cordilleran Foreland Basin through the Late Cretaceous: Examples from the Piceance and Denver Basin

Zhilin Shi (z_shi@coloradocollege.edu), Ren Carrol (r_carrol@coloradocollege.edu), and Zhiyang Li (zhiyang.li@tamu.edu)
Department of Geology, Colorado College, CO, USA

COLORADO COLLEGE

Abstract

Although flexural subsidence has long been considered the dominant mechanism of the development of the Cordilleran foreland basin (CFB), dynamic subsidence related to mantle processes has been increasingly invoked to explain the subsidence and migration of depocenters in the CFB. To determine and distinguish different subsidence mechanisms responsible for the development of CFB, detailed stratigraphic analyses of the Upper Cretaceous strata in two Laramide basins—the Piceance and Denver basins—were conducted. The profusion of well logs and previous stratigraphic investigations allow for the high-resolution reconstruction of the geo-history in these two basins through the Late Cretaceous. Seventy-six well logs were used to generate short-term, high-resolution isopach maps using IHS Petra. The stratal thickness trend observed from successive isopach maps was used as a proxy to characterize the spatial distribution of tectonic subsidence in the study area through time. The 100-80 Ma isopach maps reveal the stratal thickness increases to the east in both basins, reflecting dominant flexural subsidence caused by the loading of the Sevier thrust belt. The 80-74 Ma isopach maps show increased sediment accumulation rates and thickening trends inconsistent with the predicted flexural subsidence profile, indicating the influence of dynamic subsidence in central Colorado since ~80 Ma. The change in isopach pattern can be linked to the migration of a hypothesized oceanic plateau that flattened Farallon Plate subduction, in front of which the mantle downwelling would cause dynamic subsidence in the Piceance and Denver basins. The 74-66 Ma isopach maps point to more complex interactions of different subsidence mechanisms. The subsidence in both Piceance and Denver basins likely was strongly influenced by flexural subsidence caused by the development of Laramide-style uplifts and a component of additional dynamic subsidence during this time. High-resolution results from this study provide better constraints on the timing and effects of different subsidence mechanisms in the Late Cretaceous CFB and more detailed insights into the role of dynamic subsidence on the development of retroarc foreland basins influenced by flat-slab subduction.

1. Introduction: Subsidence Mehcanisms

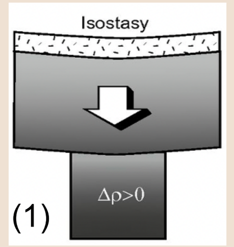

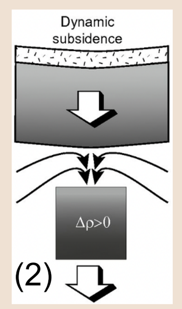

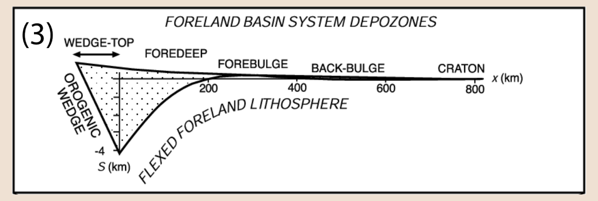

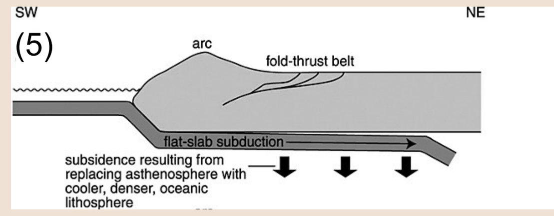

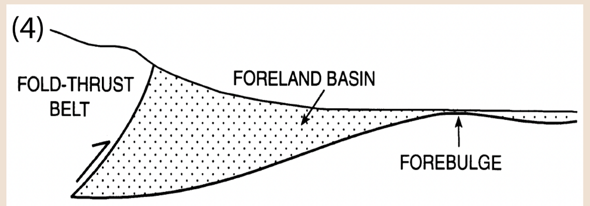

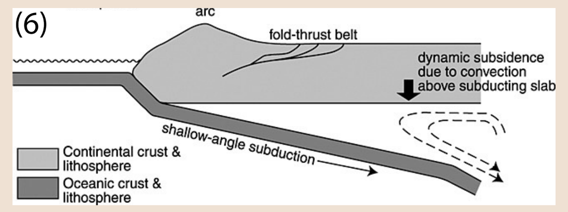

Fig. 1 and Fig. 2 Diagrams illustrating differences between isostatic (Fig. 1) and dynamic (Fig. 2) subsidence mechanisms (Heller and Liu, 2016).
Fig.3 and Fig. 4 Schematic cross section showing the four depozones in retroarc foreland basin developed under dominant flexural loading of the adjacent fold-thrust belt (DeCelles and Giles, 1996; DeCelles 2004).
Fig. 5 Subcrustal loading by a flat subducting plate causes broad wavelength subsidence proposed by Cross and Pilger (1978).
Fig. 6 Dynamic subsidence caused by downwelling mantle corner flows induced by low-angle or flat subduction of an oceanic plate (Mitrovice et al., 1989; Spasojevic et al., 2009; Liu et al., 2010 Painter and Carrapa, 2013).

Subsidence Mechanism	Flexural Subsidence	Dynamic Subsidence
Subsidence Trend	Wavelength is short to moderate (within ~200-300 km)	Wavelength is long (> 500 km)
Sediment Accumulation	Sediment is thickest adjacent to fold-thrust belt	Sediment is thickest in center of long-wavelength depocenter

2. Methodology and Study Area

Chronostratigraphic and biostratigraphic frameworks of the Upper Cretaceous Strata in the Denver and Piceance basins were first developed based on the compilation of many previous studies. Radioisotope dating of ammonite and other macrofossil biozones (Ogg et al., 2012) allows to assign numerical ages to the chronostratigraphic frameworks. The geologic time scale used in this study is from Gradstein et al. (2012). Six chronostratigraphic surfaces were selected to divide the Upper Cretaceous strata into six chronostratigraphic packages in each basin.

This study analyzes subsurface geophysical well log data in IHS Petra. Spontaneous potential log or gamma ray log and resistivity log were used to determine differences in lithology and pick formation tops across 76 wells (36 from the Piceance basin and 40 from the Denver basin). Well log data suitable for this project contain the entire Upper Cretaceous Strata, spontaneous potential or gamma ray and resistivity data. In some wells, formation tops previously picked by other researchers were used.

The stratigraphic thickness between picked chronostratigraphic surfaces were then used to generate isopach maps in IHS Petra. Isopach maps of six time intervals were developed to illustrate the spatial variations in stratal thickness, a proxy for tectonic subsidence, across the Denver and Piceance basins through the Late Cretaceous. Based on the shape and location of the depocenter, different subsidence mechanisms can be distinguished. Subsidence caused by sediment loading is removed through backstripping using four wells to better constrain the magnitude of tectonic subsidence through space and time.

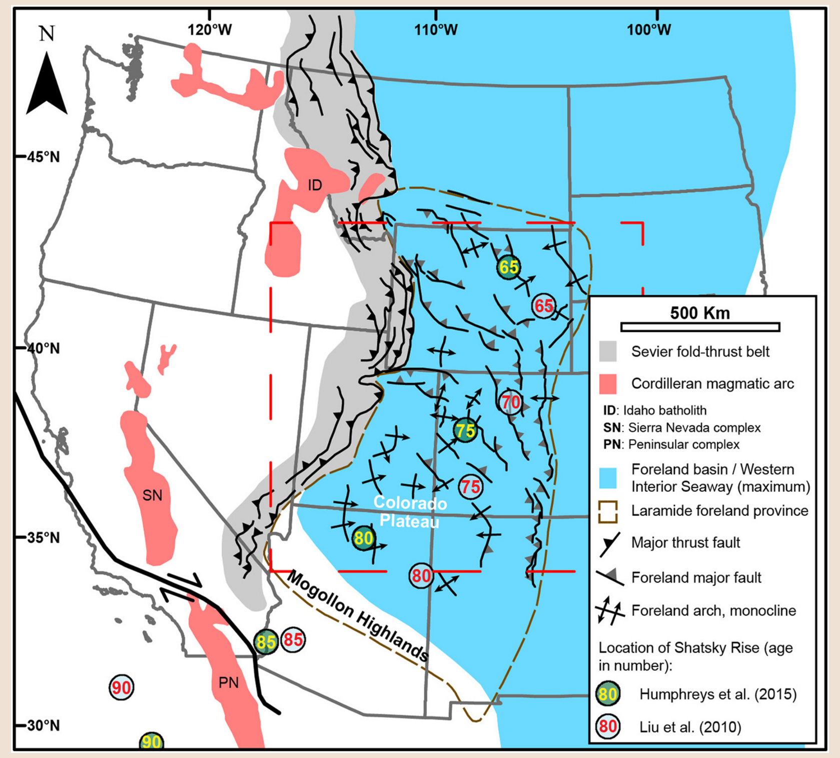

Regional index map of the western USA including the Sevier fold-thrust belt, Laramide province, and Cordilleran magmatic arc (Li and Aschoff, 2022) modified from DeCelles, 2004 and Yonkee and Weil, 2015). The inferred path of the subducted oceanic plateau, conjugate Shatsky Rise, beneath North America (modified from Humphreys et al., 2015 and Liu et al., 2010)

3. Chronostratigraphic Framework of Upper Cretaceous Strata in the Study Area

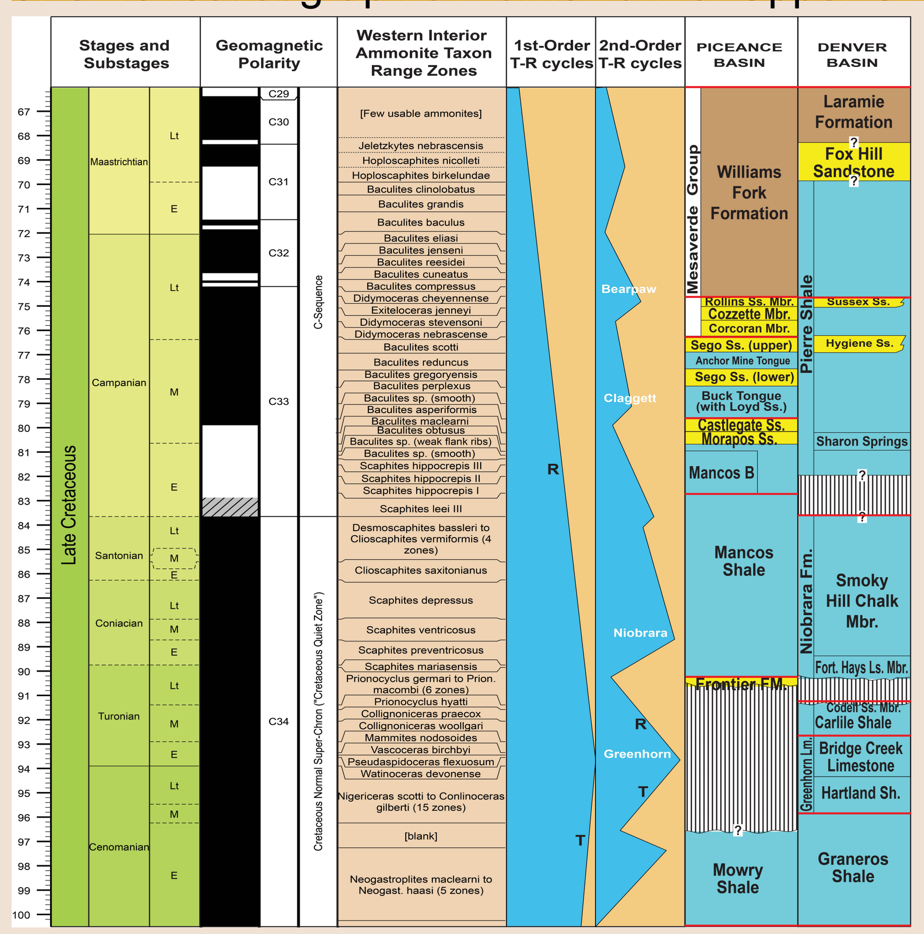

PICEANCE BASIN					DENVER BASIN				
Geologic Time Scale/Well Log Trend	Geological Formation	Ammonite Biozone	Absolute Age (Ma)	Source(s) used to trace Ammonite Biozone	Geologic Time Scale/Well Log Trend	Geological Formation	Ammonite Biozone	Absolute Age (Ma)	Source(s) used to trace Ammonite Biozone
Cretaceous top	Williams Fork (top)	Hoploscaphites nicolleti	69.30	Li (2021)	Top of Upper Cretaceous	Laramie Formation (top)	Base of Paleogene	66	Ogg et al., (2012) & Li and Aschoff, (2022)
Marked by sharp increase in GR and Res variability caused by finely interbedded sandstones and silts	Rollins (top)	Didymoceras cheyennense	74.60	Schwendeman (2011)	Late Campanian	Sussex Sandstone (top)	Base of Baculites compressus	~74.21	Izett et al., (1971) & Ogg et al., (2012)
First upward coarsening trend above buck tongue shale. Sandwiched between upward coarsening patterns of Lloyd and Corcoran Sandstones	Sego (top)	Didymoceras nebrascense	76.27	Schwendeman (2011)	Early Campanian	Niobrara Formation (top)	Base of Baculites sp. (smooth)	81.28	Ogg et al., (2012) & Joo and Sageman, (2014)
Marked by upward coarsening trend in GR data and increasing Resistivity. Both see a sharp reversal at the top of Castlegate due to mudstone progradation	Castlegate (top)	Baculites sp. (smooth)	79.64	Schwendeman (2011)	Middle Turonian	Carlile Shale (top)	between Top of Prionocyclus hyatti and Base of Prionocyclus germari	89.98	Ogg et al., (2012) & Joo and Sageman, (2014)
Distinct in the western Piceance Basin. Within Mancos shale section, marked by a distinct decrease in radioactivity.	Mancos B (base)	Scaphites leei III	83.64	Anna (2012)	Early Turonian	Greenhorn Formation (top)	Collignoniceras woollgari	~92.64	Ogg et al., (2012) & Joo and Sageman, (2014)
Appears as a thin but distinct decrease in GR and increase in Res on well log data within the thick Mancos shale segment.	Frontier (top)	Scaphites nigricollensis	90.24	Anna (2012)	Late Cenomanian	Graneros Shale (top)	Base of Plesiacanthoceras wyomingense	95.67	Ogg et al., (2012) & Joo and Sageman, (2014)
Cenomanian base	Mowry Shale (base) or Dakota (top)	Unaffiliated	100.50	Li (2021)	Base of Upper Cretaceous	Graneros Shale (base)	Mantelliceras mantelli (Tethyan zonation)	~100.25	Ogg et al., (2012)

4. Regional Isopach Patterns

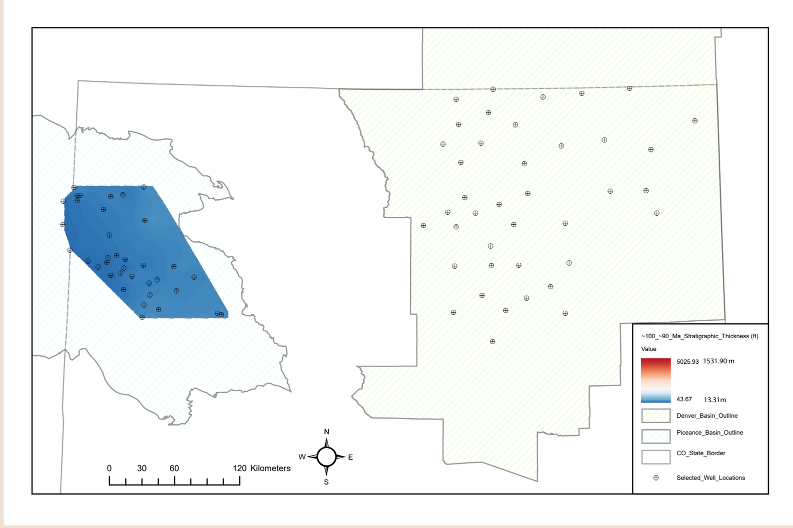

(~100 - ~90 Ma)
Low overall sediment accumulation rate and an eastward stratigraphic thickening trevnd in the Piceance basin (backbulge depozone)
Sediment accumulation rate range: 8 ft/Ma - 24 ft/Ma (2.5 m/Ma - 7.3 m/Ma)

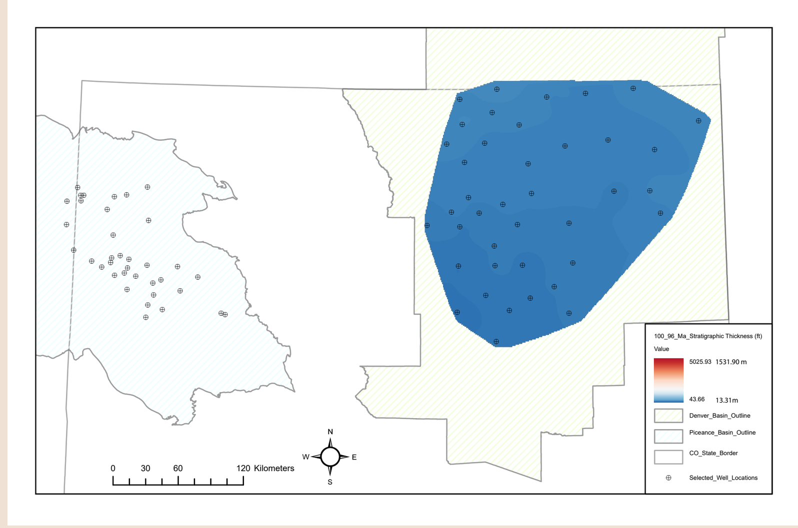

(100 - 96 Ma)
Low overall sediment accumulation rate and a slight northeastward thickening trend in strata thikcness in the Denver Basin (backbulge depozone)
Sediment accumulation rate range: 28 ft/Ma - 54 ft/Ma (8.5 m/Ma - 16.5 m/Ma)

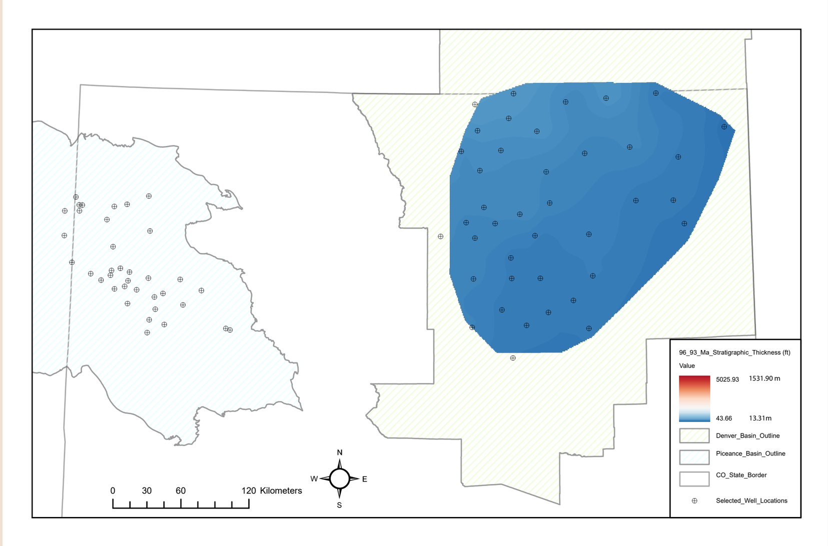

(96 - 93 Ma)
Low overall sediment accumulation rate and a northwestward stratigraphic thickening trend in the Denver Basin
Sediment accumulation rate range: 34 ft/Ma - 93 ft/Ma (10.4 m/Ma - 28.3 m/Ma)

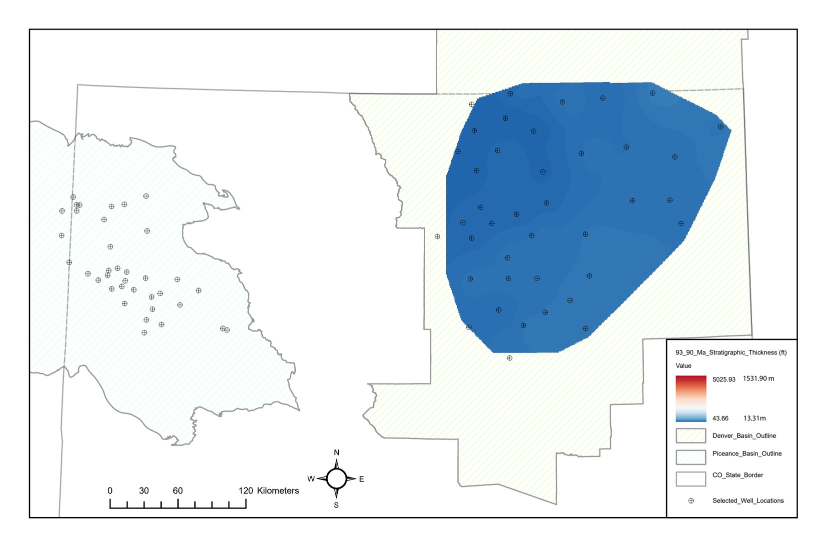

(93 - 90 Ma)
Low overall sediment accumulation rate and a southeastward stratigraphic thickening trend in the Denver Basin
Sediment accumulation rate range: 14 ft/Ma - 53 ft/Ma (4.3 m/Ma - 15.2 m/Ma)

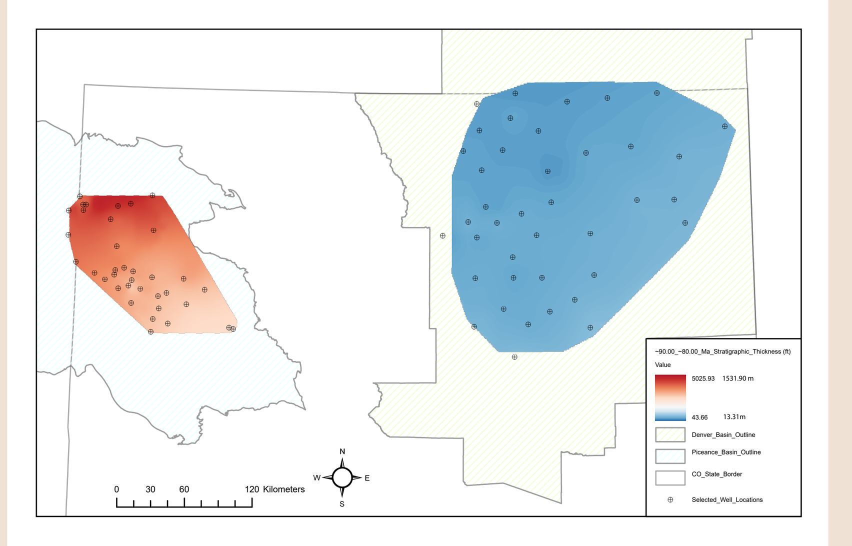

(~90 - ~80 Ma)
High overall sediment accumulation rate and a northwestward stratigraphic thickening trend in the Piceance Basin
Low overall sediment accumulation rate and a southeastward stratigraphic thickening trend in Denver Basin
Sediment accumulation rate range in PB: 217 ft/Ma - 433 ft/Ma (66.1 m/Ma - 132.0 m/Ma)
Sediment accumulation rate range in DB: 31 ft/Ma - 66 ft/Ma (9.4 m/Ma - 20.1 m/Ma)

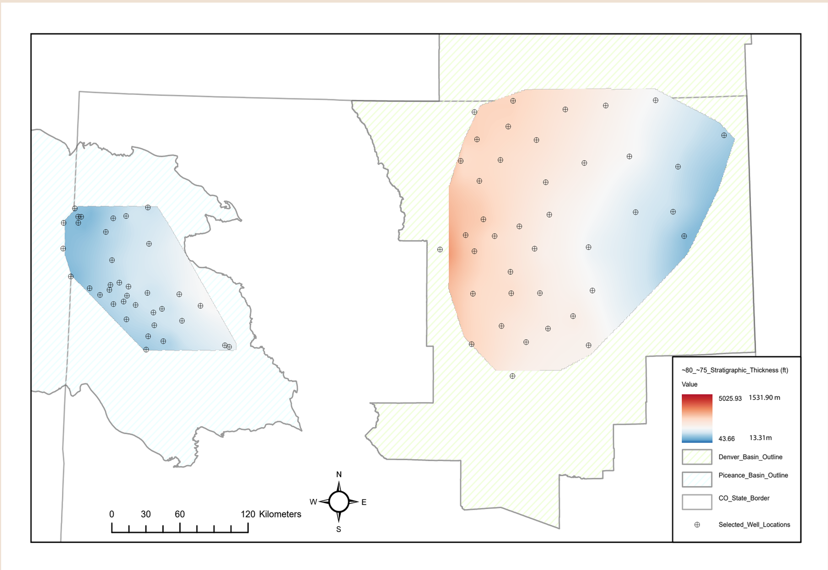

(~80 - ~75 Ma)
High overall sediment accumulation rate and an eastward stratigraphic thickening trend in Piceance Basin
High overall sediment accumulation rate and a westward stratigraphic thickening trend in Denver Basin
Sediment accumulation rate range in PB: 182 ft/Ma - 533 ft/Ma (55.5 m/Ma - 162.5 m/Ma)
Sediment accumulation rate range in DB: 82 ft/Ma - 477 ft/Ma (25.0 m/Ma - 145.4 m/Ma)

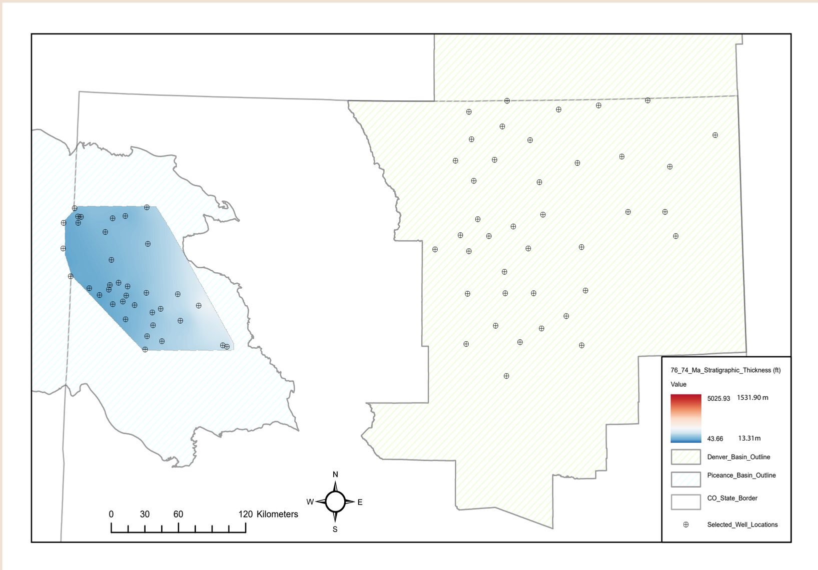

(76 - ~74 Ma)
High overall sediment accumulation rate and an eastward stratigraphic thickening trend in the Piceance Basin
Sediment accumulation rate range:168 ft/Ma - 707 ft/Ma (51.2 m/Ma - 215.5 m/Ma)

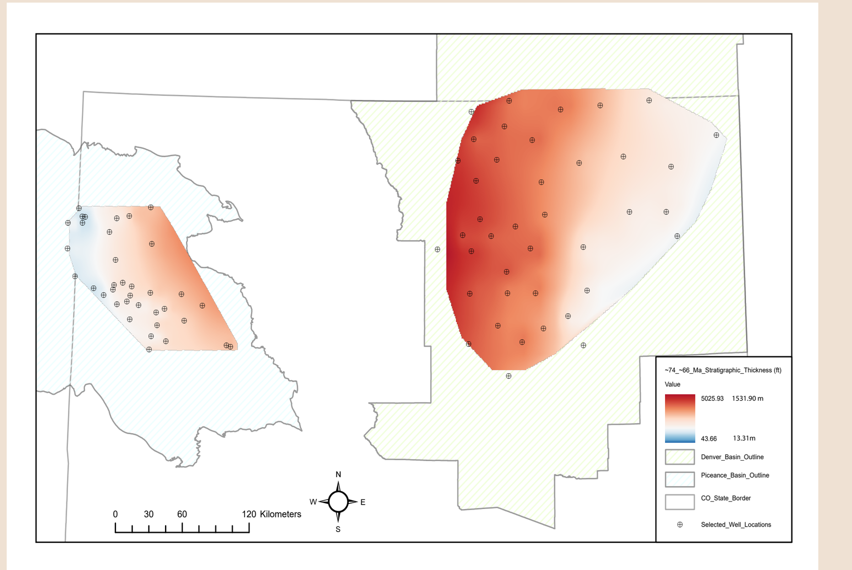

(~74 - ~66 Ma)
High overall sediment accumulation rate and an eastward stratigraphic thickening trend in Piceance Basin
High overall sediment accumulation rate and a westward stratigraphic thickening trend in Denver Basin
Sediment accumulation rate range in PB: 120 ft/Ma - 436 ft/Ma (36.6 m/Ma - 133.2 m/Ma, lowered than 80-74 Ma)
Sediment accumulation rate range in DB: 165 ft/Ma - 628 ft/Ma (50.3 m/Ma - 191.4 m/Ma)

5. Backstripping Results from Piceance and Denver Basin

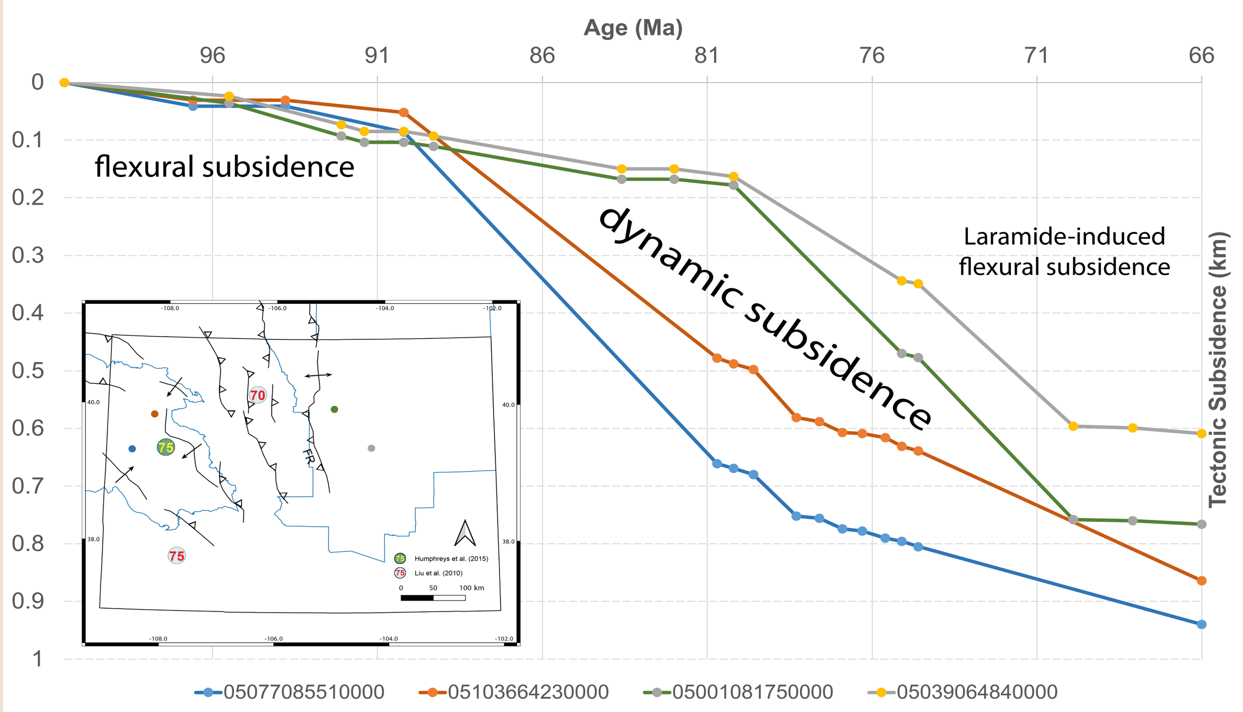

Tectonic subsidence curves in the Piceance and Denver basins developed through 1D backstripping using two wells from each basin. Flexural subsidence is the dominant subsidence mechanism in both basins during 100-90 Ma. Dynamic subsidence started to influence Piceance basin earlier (at ca. 90 Ma) and Denver basin later (at ca. 80 Ma).

6. Conclusion

From the beginning of Late Cretaceous (ca. 100 Ma) to late Turonian (ca. 90 Ma), both basins experienced dominant flexural subsidence induced by loading of the Sevier thrust belt developed in response to the subduction of the Farallon oceanic plate beneath the North American Plate. Both Denver and Piceance basins were located at the backbulge depozone. Being in the closer proximity to the forebulge, Piceance basin experienced less flexural subsidence compared to the Denver basin (up to ~ 10 m/Ma).

From late Turonian (~ca. 90 Ma) to early Campanian (~ca. 83 Ma), the Piceance Basin started to undergo dynamic subsidence. The stratigraphic thickness and sediment accumulation rate (up to ~ 130 m/Ma) in Piceance basin increased significantly. The tectonic subsidence (dominantly dynamic subsidence) rate in the Piceance basin is up to 65 m/Ma. Denver Basin was not located at the depocenter during this time and had not significantly influenced by the dynamic subsidence yet. This is consistent to the reconstructed northeastward trajectory of the conjugate Shatsky Rise.

From early Campanian (~ca. 83 Ma) to late Campanian (~ca. 72 Ma), the area of dynamic subsidence caused by the conjugate Shatsky Rise has shifted away from the Piceance Basin and started to influence the Denver basin. The stratigraphic thickness and sediment accumulation rate escalated in Denver basin. The tectonic subsidence (dominantly dynamic subsidence) rate in the Denver basin is up to ~ 60 m/Ma, comparable to the tectonic subsidence rate Piceance basin experienced during 90 to 83 Ma.

Another important tectonic event, Laramide Orogeny, likely took place and started to influence our study area since the late Campanian (~ca. 72 Ma). The uplift of the Front Range west of Denver basin likely contributed to a component of flexural subsidence in Denver basin. Dynamic subsidence is interpreted to have still played a role, considering the abnormally thick stratal thickness in Denver basin during 72 Ma to 66 Ma. Laramide-style structures adjacent to Piceance are generally considered younger than the Late Cretaceous. Thus, the still fairly rapid tectonic subsidence in the Piceance basin (up to 30 m/Ma) can be attributed to dynamic subsidence. The tectonic subsidence (dominantly dynamic subsidence) rate in both Denver and Piceance basins decreased since ca. 72 Ma, which can be linked to the arrival of the still relatively buoyant conjugate Shatsky rise during this time.

Implications for Future Work

1. Small areas have more fine timelines to pick due to good consistence of geologic formations.

2. To better understand the different tectonic subsidence, more detailed stratigraphic studies form other segmented CFB can be done in the future.

3. The findings from this basin can be used to study other basins across the globe.

Acknowledgement

We are thankful of the Colorado College Geology Department for access to the software, facilities, and instructor that gave us the opportunity to pursue this work.

We are grateful to the past researchers for providing valuable datasets that made this project possible.

We also appreciate IHS Marki (now a part of S&P Global) for donating the license of Petra through the University Grant Program.

Finally, thank you to Professor Li. (Texas A&M International University) who provided strong support and instruction throughout our research project.